Fundamental Studies of Molecular Interactions and Dissolution Inhibition in Poly(norbornene-*alt*-maleic anhydride)-Based Resins

F. M. Houlihan,* G. Dabbagh, I. Rushkin,† R. Hutton, D. Osei,‡ J. Sousa,§ K. Bolan, O. Nalamasu, and E. Reichmanis

Bell Laboratories, Lucent Technologies, 600 Mountain Avenue, Murray Hill, New Jersey 07946

Z. Yan and A. Reiser

Institute of Imaging Science, Polytechnic University, Brooklyn New York 11201

Received May 10, 2000. Revised Manuscript Received September 6, 2000

The progress of developer base into films of terpolymers of norbornene−maleic anhydride and acrylic acid was shown to be a percolation process with a critical site concentration of $x(c) = 0.084$, implying that every acrylic acid site in the terpolymer makes 12 monomer units of the polymer water compatible. Using these terpolymers, the dissolution inhibition mechanism for two types of common additives, *tert*-butyl carboxylate (e.g., cholates, cyclohexanecarboxylates, and malonates) dissolution inhibititors and onium salt photoacid generators (PAG's), were examined. Additionally, the dissolution promotion mechanism of carboxylic acids released from acidolysis of *tert*-butyl esters was investigated. For a wide range of cholates and other *tert*-butyl carboxylate derivatives, increasing hydrophobicity is a good predictor of increased dissolution inhibition. The molar dissolution promotion ability of a carboxylic acid increases with increasing number of both carboxyl and hydroxyl ester functional groups. For onium salt PAG's, a decrease in dissolution inhibition occurred when increasing the hydrophobicity and size of counteranions. Rather than being tied to hydrophobicity, large changes of dissolution inhibition in this class of materials appear to correlate with their ability to interact with carboxyl groups.

Introduction

Advancements in microelectronics technology have been enabled by materials chemistry in general and polymer chemistry in particular. Over the past several decades, device complexity and functionality have increased while the minimum feature size of individual circuit elements has dramatically decreased. This trend is predicted to continue well into the next decade and is critically dependent upon the technologies involved in delineating the circuit pattern. Perhaps the key variable affecting feature size resolution is the wavelength of light used for exposure. The introduction of 248 nm lithography required the first revolutionary change in imaging materials. The materials design had to effectively boost the limited photon flux from the exposure tool. This was achieved through having the resist initiate a cascade of chemical reactions (chemical amplification).[1] Devices with minimum dimensions as small as 0.1 μm are expected to be manufactured through lithographic technologies employing 193 nm ArF excimer laser light as the exposure source. The success of 193 nm lithography has hinged on the design, development, and implementation of patternable, polymer-based materials. Families of 193 nm transparent polymer matrices based on methacrylate and alicyclic backbone chemistries have been developed to maximize lithographic performance with minimal sacrifice in etching resistance.[2,5]

For the class of materials based on alternating copolymers of norbornene (NB) and maleic anhydride (MA), in which acrylate "defects" are introduced via free

† Presently at Arch Chemicals Inc., East Providence, RI 02914.

‡ Summer student presently at Princeton University, Princeton, NJ.

§ Summer student presently at the New Jersey Institute of Technology, Newark, NJ.

(1) For some lead in references on chemically amplified resists, see: Reichmanis, E.; Houlihan, F. M.; Nalamasu, O.; Neenan, T. X. *Chem. Mater.* **1991**, *3*, 397.

(2) For some lead in references on 193 nm resists, see: (a) Allen, R. D.; Wan, I. Y.; Wallraff, G. M.; DiPietro, R. A.; Hofer, D. C.; Kunz, R. R. *J. Photopolym. Sci. Technol.* **1995**, *8*, 623. (b) Nakano, K.; Maeda, K.;. Iwasa, S.; Ohfuji, T.; Hasegawa, E. *Proceedings of the International Society for Optical Engineering; Advances in Resist Technology and Processing XII* **1995,** *2438*, 433−440. (c) Nozaki; N.; Kaimoto; Y.; Takahashi; M.; Takeshi; S.; Abe N. *Chem. Mater.* **1994**, *6*, 1492−1498.

(3) Wallow, T. I.; Houlihan, F. M.; Nalamasu, O.; Chandross, E. A.; Neenan, T. X.; Reichmanis, E. *Proceedings of the International Society for Optical Engineering; Advances in Resist Technology and Processing XIII* **1996**, *2724*, 355.

(4) (a) Houlihan, F. M.; Kometani, J. M.; Timko, A. G.; Timko, R. S.; Cirelli, R. A.; Reichmanis, E.; Nalamasu, O.; Gabor, A. H.; Medina, A. N.; Biafore, J. J.; Slater, S. G. *J. Photopolym. Sci. Technol.* **1998**, *11*, 419. (b) Houlihan, F. M.; Timko, A.; Hutton, R.; Cirelli, R.; Kometani, J. M.; Reichmanis, E. 193 nm Single Layer Resist Based on Poly(norbornene-*alt*-maleic anhydride) Derivatives. In *Micro and Nanopatterning Polymers*; Reichmanis, E., Nalamasu, O., Ueno, T., Eds.; ACS Symposium Series 706; American Chemical Society: Washington, D.C., 1998; Chapter 15, p 191.

(5) Reichmanis, E.; Nalamasu, O.; Houlihan, F. M.; Wallow, T. I.; Timko, A. G.; Cirelli, R.; Dabbagh, G.; Hutton, R. S.; Novembre, E. A. *J. Vac. Sci. Technol.* **1997**, *B15* (6), 2528.

10.1021/cm000385k CCC: $19.00
Published on Web 10/28/2000

radical polymerization, use of a photoacid generator (PAG) can induce image formation when an acid-cleavable moiety is present on the polymer.[3,4] However, the performance of the resist can be significantly improved through the use of a dissolution inhibitor (DI). Building upon early work using 2-nitrobenzylcholate as a dissolution inhibitor for methacrylate and methacrylic acid copolymers,[6,7] several dissolution inhibitor candidates based upon cholate ester chemistry have been identified for 193 and 248 nm resist applications.[8−12] Analogously, Ito et al.[13] showed that onium salt PAG components also act as dissolution inhibitors in phenolic resins patternable at 248 nm. Consequently, identifying the factors that are important in determining the effectiveness of both cholate esters and PAG's as dissolution inhibitors in 193 nm polymer resins is a subject of critical importance. Factors that may contribute to the effectiveness of these additives as dissolution inhibitors may include their hydrophobicity and their ability to undergo inter- and intramolecular interactions in the polymer matrix.

Here, dissolution rate measurements were coupled with Fourier transform infrared (FT-IR) and nuclear magnetic resonance (NMR) spectroscopic characterization and traditional cloud point determinations to study the nature of the mechanism for dissolution inhibition in blends of either *tert*-butyl carboxylate esters or onium salt PAG's with poly(norbornene-*alt*-maleic anhydride-*co*-acrylic acid) P(NB/MA/AA). This study reveals that the nature of the mechanism for dissolution inhibition of onium salt PAG's differs greatly from that of cholate and other carboxylate esters and elucidates material design options for enhanced performance.

Results and Discussion

The Mechanism of Polymer Dissolution in Aqueous Base. Study of the dissolution rate of P(NB/MA/AA) terpolymers containing differing amounts of the acrylate component in 0.26 N aqueous tetramethylammonium hydroxide (TMAH) confirmed that the dissolution proceeds via a percolation process. Percolation theory predicts a quadratic relation between the dissolution rate and the percolation site concentration, corrected for a critical minimum site concentration below which dissolution no longer occurs (eq 1), where x_{AA} is the mole fraction of acrylic acid (AA) groups in the polymer, $x_{AA}(c)$ is the critical minimum mole fraction of AA, and R is the dissolution rate of the film.[14]

$$R = \alpha[x_{AA} - x_{AA}(c)]^2 \qquad (1)$$

For P(NB/MA/AA), the dissolution rate was found to have a quadratic dependence on the concentration of ions sites (Figure 1) in which α was 61.7 and $x_{AA}(c)$ = 0.084. This implies that a single acrylate (AA−) ionic site can make approximately 12 monomer units (i.e., $1/x_{AA}(c)$ = ∼12) of the material compatible with the aqueous developer. Having established the mechanism for polymer dissolution, it is now possible to formulate a schematic representation of the dissolution process.

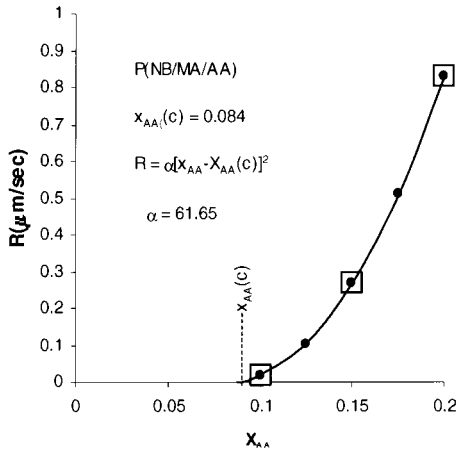

Figure 1. Dependence of dissolution rate on the concentration of ionizable sites in the matrix. The molfraction of these ion sites is (x_{AA}). The critical mole fraction of ion sites below which the film does not dissolve is $x_{AA}(c)$ = 0.084.

If a resin film containing carboxylic moieties is immersed in an alkaline developer, the base entering the film encounters AA groups and converts them into (AA−) ion sites. When a base anion (OH−) encounters an acid site, the proton of the acid and the base anion combine to form a molecule of water, and at that point the path of that particular base ion comes to an end. The cation of the base (e.g., K^+ or TMA^+) associates itself with the carboxylate ion, and the two together form a resin bound ion-pair site. A thin penetration zone of ion pairs is gradually formed at the interface with the developer. The rate of travel of the zone is equal to the dissolution rate of the polymer film, R, defined as the loss of thickness in unit time (measured e.g., in μm/s or A/s).[15,16] Figure 2 shows a schematic depiction of the movement of the penetration zone into the bulk of a carboxylic acid matrix resulting in dissolution of the resin. It is conceivable that the MA unit could undergo hydrolysis during this process, forming carboxylic acids thereby contributing additional percolation sites. This matter will be discussed latter during the section of the paper devoted to studies of dissolution promotion.

Mechanism for Dissolution Inhibition and Promotion in Poly(NB/MA/AA)-Based Resins. It can readily be seen that incorporating additional components such as *tert*-butyl carboxylate esters and onium salt based photoacid generators would affect the dissolution process. In a simple model, one could view either of these components as an obstacle to the move-

(6) Reichmanis, E.; Wilkins, C. W., Jr.; Chandross, A. E. *J. Vac. Sci Technol.* **1981**, *19* (4), 1338.
(7) Wilkins, C. W., Jr.; Reichmanis, E.; Chandross, A. E. *J. Electrochem. Soc.* **1982**, *129* (11), 2552.
(8) O'Brien, M. J. *Polym. Eng. Sci.* **1989**, *29*, 846.
(9) Crivello, J. V. *Chem. Mater. Sci.* **1994**, *6*, 2167.
(10) Allen, R. D.; Wan, I. Y.; Wallraff, G. M.; Di Pietro, R. A.; Hofer, D.; Kunz, R. R. *J. Photopolym. Sci Technol.* **1995**, *8*, 623.
(11) Houlihan, F. M.; Wallow, T.; Timko, A.; Neria, E.; Hutton, R.; Cirelli, R.; Nalamasu, O.; Reichmanis, E. *Proceedings of the International Society for Optical Engineering; Advances in Resist Technology and Processing XIV* **1997**, *3049*, 84.
(12) Houlihan, F. M.; Wallow, T.; Timko, A.; Neria, E.; Hutton, R.; Cirelli, R.; Kometani, J. M.; Nalamasu, O.; Reichmanis, E. *J. Photopolym. Sci. Technol.* **1997**, *10*, 511.
(13) Ito, H.; Fenzel-Alexander, D.; Breyta, G. *J. Photopolym. Sci. Technol.* **1997**, *10* (3), 397.
(14) For lead in references to percolation theory and its application to resist dissolution, see, respectively: (a)Essam J. M. *Rep. Prog. Phys.* **1980**, *43*, 53. (b) Yeh T. F.; Shih H. Y.; Reiser, A. *Macromolecules* **1992**, *25*, 5345.
(15) Reiser, A.; Shih, H. Y.; Yeh, T. F.; Huang, J. P. *Angew. Chem., Int. Ed. Engl.* **1996**, *35*, 2429.
(16) Reiser, A. *J. Imaging Sci. Technol.* **1998**, *42*, 15.

Table 1. Properties of Select *tert*-Butyl Carboxylate DI's

DI entry[a] no.	f^b (*f*(molar))	cloud point	M_W	Log P_{oct}[c]	entry no. free carboxyl ic acid[d]	free acid *f* (*f*(molar))[b]	Δ*f* (Δ*f* molar)	R_{max} (A/s)[e]	contrast[c]
1	1.3 (0.60)	36	464.7	4.31	**1a**	−3.9(−1.59)	5.2(−2.20)	2560	8.4
2	2.3(1.0)	50	448.7	6.35	**2a**	−3.5(−1.37)	5.8(2.41)	1730	10
3	6.0(2.6)	73	432.7	8.4	**3a**	−2.8(−1.05)	8.8(3.65)	1350	32
4	2.6(1.8)	55	448.7	6.34					
5	7.4(7.1)	91	961.5	18.89					
6	2.9(2.9)	56	1025. 5	10.71	**6a**	−3.43(−3.1)	6.28(6.05)	2160	10
7	5.1(1.5)	46	284.4	3.88	**7a**	−5.0(−0.86)	10.1(2.31)	3000	27
8	5.0(1.4)	52	284.4	3.84	**8a**	−4.7(−0.80)	9.7(2.23)	2830	45
9	3.8(1.5)	56	384.5	4.52	**9a**	−6.3(−1.36)	10.1(2.82)	>6000	32
10	2.9(0.68)	55	236.3	4.29	**10a**	−4.6(−0.82)	7.43(1.51)		
11	3.6(0.78)	ND	216.3	2.10					
12	5(1.36)	ND	272.4	4.04					
13	1.4(0.28)	ND	202.2	2.43					
14	2(0.52)	ND	258.3	3.52					
15	4.6(1.1)	ND	240.4	5.55					

[a] Assignment of *tert*-butyl carboxylate DI's as follows: 1, *tert*-butyl cholate; 2, *tert*-butyl deoxycholate; 3, *tert*-butyl lithocholate; 4, *tert*-butyl chenodeoxycholate; 5, bis(*tert*-butyl 3α-yl-cholan-24-oate) glutarate; 6, bis(*tert*-butyl 3α-yl,7α,12α-5*β*-dihydroxycholan-24-oate) glutarate; 7, di-*tert*-butyl 1,4-cyclohexanedicarboxylate; 8, di-*tert*-butyl 1,3-cyclohexanedicarboxylate; 9, tri-*tert*-butyl 1,3,5-cyclohexanetricarboxylate; 10, *tert*-butyl adamantanecarboxylate; 11, di-*tert*-butyl malonate; 12, di-*tert*-butyl butylmalonate; 13, *tert*-butyl oxylate; 14, di-*tert*-butyl acetonedicarboxylate; 15, *tert*-butyl *trans*-4-cyclohexanecarboxylate. [b] Dissolution inhibition factors (*f*) were measured in a poly(NB/MA/AA) resin containing 12.5% AA; values of *f* are measured by finding the slope of the graph of log(*R*) vs wt % and multiplying it by −100. [c] See ref 20. [d] **E**ntry numbers with "a" denotation correspond to the free acid of the corresponding DI number (e.g., 1a = cholic acid [3α-7α,12α-5*β*-trihydroxycholan-24-oic acid]). [e] R_{max} and contrast were measured for dissolution in 0.26 N tetramethylammonium hydroxide using a dissolution rate monitor for a resist formulated with P(NB-MA-AA-TBA) quaternary polymer containing 25 wt % of dissolution inhibitor, 2 wt % bis(*tert*-butylphenyliodonium) nonaflate, flood exposed to 100 mJ/cm^2 at 193 nm and baked at 150 °C for 90 s and developed in 0.26 N TMAH.

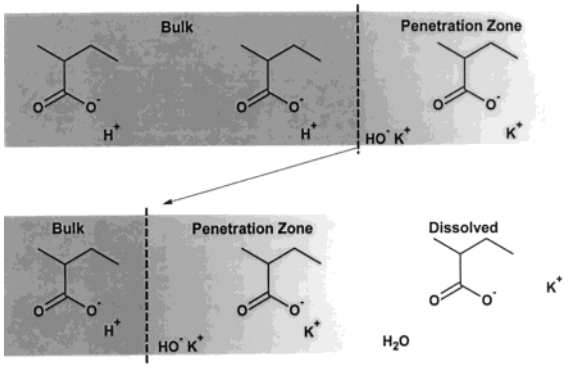

Figure 2. Schematic depiction of the movement of the penetration zone.

ment of aqueous base solution from one percolation site to another. Consequently, both the hydrophobicity of an additive and the strength with which it interacts with the matrix would be expected to play a role in retarding percolation (i.e., affect dissolution inhibition).

To quantify the dissolution inhibition effect of both classes of materials, the inhibition factors of these materials were determined in a P(NB/MA/AA) resin containing 12.5% of the acrylic acid component (12.5% AA). This was done by first preparing resin films containing increasing quantities of the additives and then measuring their dissolution rates (*R*). The dissolution inhibitor factor (*f*) is derived from the slope (i.e., $f = -100 \times$ slope) of the plot of log(*R*) vs the wt % of materials in a film (Meyerhofer plot).[17] Values of *f* were found for a number of additives including *tert*-butyl cholates, other *tert*-butyl carboxylates, and onium salts (Tables 1 and 2). Table 1 also lists the dissolution promotion factors found for the parent carboxylic acids derived from select *tert*-butyl carboxylates. Finally, *f* has been adjusted to a molarity scale [$f \times M_W/1000 = f$(molar)].

Dissolution Inhibition Mechanism of Cholate Dissolution Inhibitors. Cholate ester dissolution inhibitors are able to interact with the matrix via a number of sites. Notably, cholate hydroxyl moieties could interact with polar moieties on the matrix resin blocking their availability and thus the ability of the composite film to dissolve in the aqueous media. Alternatively, these moieties could interact with the matrix binding the hydrophobic steroidal polycyclic moiety better to the polymer matrix. This later behavior would be analogous to the manner in which electron-rich sulfonate pendant groups help diazonaphthoquinone dissolution inhibitors better interact with novolak resins[17b] and act as potent dissolution inhibitors.

This view was inspired by the general behavior of the steroids, of which cholates are a subclass. Steroids affect a great number of biological functions in very specific ways, which suggest that they are able to recognize the chemical and steric structure of various receptor sites in biological systems.[18] It is tempting to look for such a mechanism in the materials described here. The nature of different interactions in such systems was broken up by doing experiments in which different cholate DI's were evaluated in three polymer matrices based upon P(NB/MA/AA), poly(norbornene−maleic anhydride−*tert*-butyl acrylate) [P(NB/MA/TBA] and poly(norbornene−maleic anhydride) [P(NB/MA)]) by using FT-IR spectroscopy. These studies indicate that for a given class of cholate derivatives with similar structures, the interactions that correlate the best with the observed *f*(molar) values are interactions of hydroxyls with MA units and not interactions between carboxylic acid and MA moieties as previously hypothesized.[19] Generally speaking, the intensity of such interactions correlates

(17) (a) Dammel, R. *Diazonaphththoquinone-Based Resist;* O'Shea, Donald C., Ed.; SPIE Optical Engineering Press: Bellingham, WA, 1993; p 70 (b) Ibid. p 80.

(18) Walliman, P.; Marti, T.; Fuerer, A.; Diederich, F. *Chem Rev.* **1997**, *97*, 1567−1608.

Table 2. Properties of Select Photoacid Generators

entry no. PAG[a]	*f* (*f*(molar))[b]	cloud point	M_W	C-13 shift acetic acid (ppm)	C-13 shift dimethyl succinic anhydride (ppm)[c]
PAG1	6.9(4.7)	24.8	692.4	175.8	177.3 and 169.6
PAG2	10.2(6.5)	2.0	640.4		
PAG3	3.0(2.7)	40.3	892.4	175.9	177.3 and 169.6
PAG4	13.6(6.0)	3.0	440.1		
PAG5	12.2(6.6)	4.0	542.4	175.6	177.3 and 169.6
PAG6	13.7(7.6)	4.0	556.4		
PAG7	3.4(2.5)	41.6	730.8	175.1	
PAG8	5.3(3.6)	28.0	678.8	174.2	
PAG9	7.2(3.7)	26.3	518.5	175.9	
PAG10	7(4.1)	28.1	580.8	175	
PAG11	2(1.9)	52.0	930.8	175.1	
PAG12	6.8(5.0)	51.0	742.6		
PAG13	11.6(7.2)	80.6	624.6		

[a] PAG1, bis(*tert*-butylphenyl)iodonium nonaflate; **PAG2**, bis(*tert*-butylphenyl)iodonium perfluorobenzenesulfonate; **PAG3**, bis(*tert*-butylphenyl)iodonium perfluorooctanesulfonate; **PAG4**, bis(*tert*-butylphenyl)iodonium tetrafluoroborate; **PAG5**, bis(*tert*-butylphenyl)-iodonium triflate; **PAG6**, bis(*tert*-butylphenyl)iodonium tresylate; **PAG7**, tris(*tert*-butylphenyl)sulfonium nonaflate; **PAG8**, tris(*tert*-butylphenyl)sulfonium perfluorobenzenesulfonate; **PAG9**, tris(*tert*-butylphenyl)sulfonium tetrafluoroborate; **PAG10**, tris(*tert*-butylphenyl)sulfonium triflate; **PAG11**, tris(*tert*-butylphenyl)sulfonium perfluorooctanesulfonate; **PAG12**, bis(2,6-dinitro-α-ethyloxycarbonylbenzyl) 1,3-benzenesulfonate; **PAG13**, bis(*tert*-butylphenyl)iodonium camphorsulfonate. [b] *f* values were measured in a P(NB-MA-AA) resin with 12.5% AA using various PAG's and are established from the slope of the log(*R*) vs wt % (−slope × 100). [c] The starting peak positions for dimethyl succinic anhydride in $CDCl_3$ are 177.2 and 169.4 ppm.

with the availability of the hydroxyl moiety rather than with the number of hydroxyl groups available. For example, *tert*-butyl lithocholate possesses a hydroxyl group that is relatively unhindered and can participate well in interactions. In *tert*-butyl cholate the same hydroxyl moiety is less available owing to intramolecular hydrogen bonding, and although two other hydroxyl moieties are available these are hindered in nature and also exhibit intramolecular hydrogen bonding.[19]

Relationship between Hydrophobicity and Dissolution Inhibition for *tert*-Butyl Carboxylates. The model involving interaction between the hydroxyl of the cholate DI's and maleic anhydride repeat units does not account for all the factors contributing to dissolution inhibition since other DI's having no hydroxyl whatsoever display exceptional performance. For example bis(*tert*-butyl 3α-yl-cholan-24-oate) glutarate (*tert*-butyl lithocholate glutarate dimer) (*f*(molar) = 7.1) is 5−10 times more effective as a dissolution inhibitor compared to the *tert*-butyl cyclohexanecarboxylates and di-*tert*-butyl malonates. These latter materials in turn all have somewhat higher effectiveness at dissolution inhibition (2.5−1.3 times) than *tert*-butyl cholate (Table 1). The high dissolution inhibition of *tert*-butyl carboxylates lacking hydroxyl moieties suggests that hydrophobicity could also be playing a role. Accordingly, log P_{oct}, a measure of hydrophobicity,[20] was plotted against *f*(molar) (Figure 4). The good correlation ($R^2 = 0.92$) of this plot implies that hydrophobicity is more important than OH interactions in explaining large changes in dissolution inhibition. However, this does not mean that the molecular interactions do not play any role in explaining large changes in dissolution inhibition. Specifically, van der Waals or Debye type interactions between the *tert*-butyl carboxylates and the resin might predicate how effectively a given hydrophobic moiety will induce dissolution inhibition. In fact, the strength of complexations of many steroidal molecules with substrates[18] is known to increase with increasing log P_{oct}. For example, it has been found that the binding affinity of different cyclophanes[21] and cyclodextrin molecules[22] to a variety of cholate derivatives decreases with the increasing number of polar substituents on the cholate. Thus for these materials it is not the polar attractive interactions that but rather van der Waals surface contact and

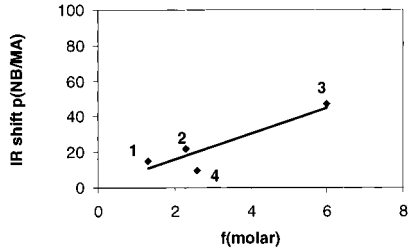

Figure 3. Plot of the IR shifts of the OH band of monomeric hydroxyl bearing cholates in a P(NB/MA) resin versus *f*(molar) measured for these materials in a P(NB/MA/AA) (12.5%) resin developed with 0.26 N TMAH.

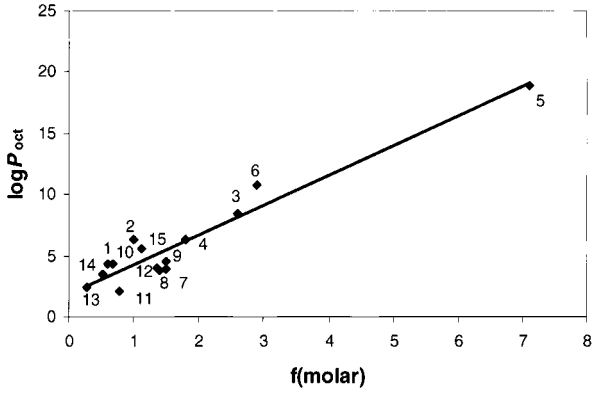

Figure 4. Plot of log P_{oct} versus *f*(molar) measured for *tert*-butyl carboxylates in a P(NB/MA/AA) (12.5%) resin developed with 0.26 N TMAH.

(19) (a) Dabbagh, G.; Houlihan, F. M.; Rushkin, I.; Hutton, R. S.; Nalamasu, O.; Reichmanis, E.; Gabor, A. H.; Medina, A. N. *Proceedings of the International Society for Optical Engineering; Advances in Resist Technology and Processing XVI* **1999**, *3678*, 86. (b) Dabbagh, G.;. Houlihan, F. M.; Rushkin, I. Hutton, R. S.;. Nalamasu, O.;. Reichmanis, E.; Gabor, A. H., Medina; A. N. Proceedings of the ACS PMSE Division, Fall Meeting, August 22−26, 1999; American Chemical Society: Washington, D.C., 1999; Vol. 81, p 53.

(20) Log P_{oct} values cited in this paper were calculated using the program ACD/log P_{oct} DB version 4.06 from Advanced Chemical Development. For a lead in reference on log P_{oct}, see: Hansch, C.; Leo, A. *Substitution Constants for Correlation Analysis*; Wiley Interscience: New York, 1979; p 13.

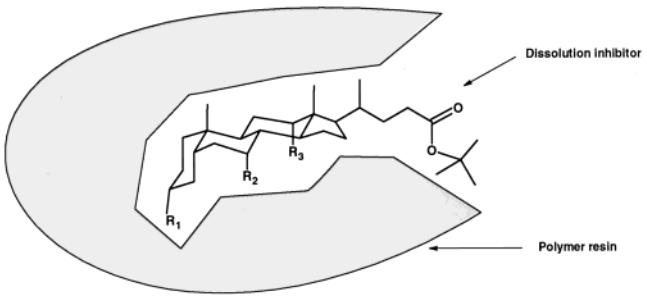

Figure 5. Illustration of complexation of a cholate dissolution inhibitor with a poly(norbornene−maleic anhydride−acrylate) matrix. R_1, R_2, and R_3 are substituents that can be either H or a polar group such as OH. Increasing OH substitution will disfavor complexation DI from the matrix. Conversly, increasing the polarizable surfaces available for van der Waals contact between the DI and the matrix favors complexation.

complexation-induced desolvation of polar groups that predicate binding selectivity. Figure 5 illustrates a similar situation that might occur for the interaction of the cholate dissolution inhibitors with the P(NB/MA/AA) matrix, where a DI with a large van der Waals surface and few polar groups would be expected to be the most effective in associating with P(NB/MA/AA), increasing its potency as a dissolution inhibitor. Another method that was used evaluate hydrophobicity is cloud point determination.[23] The cloud point values measured for a group of DI's consisting of monomeric and dimeric cholates *tert*-butyl esters, *tert*-butyl cyclohexanecarboxylates, and *tert*-butyl adamantanecarboxylate are listed in Table 1. Adjusting the cloud points to molarity (i.e., cloud point $\times$ $M_W/1000$ = cloud point(molar)) and plotting these against *f*(molar) gives a good correlation (Table 1) similar to that found for the plot with log P_{oct} (i.e., $R^2 \sim 0.90$), showing that these two measures of hydrophobicity have similar predictive value. If the cloud point(molar) vs *f*(molar) plot is restricted to cholate derivatives, the correlation improves considerably ($R^2 = 0.98$). This is perhaps because this class of materials sharing a common structural framework has similar van der Waals and/or Debye interactions with the resin.

The Contrast-Producing Event in *tert*-Butyl Carboxylates. One would expect that the dissolution promotion ability of a given carboxylic acid as measured by *f*(molar) would tend to increase with the number of carboxylic acid moieties per molecule. However, this appears to be true only when comparing carboxylic acids with similar structures. For instance, bis(3α-yl,7α,12α-5β-dihydroxycholan-24-oic acid) glutarate (cholic acid glutarate dimer), which has two carboxyl groups per molecule, has an *f*(molar) value about twice that of the monofunctional cholic acids (Table 1). Similarly, 1,3,5-cyclohexanetricarboxylic acid is 1.5 times more powerful as a dissolution promoter compared to the two cyclohexanedicarboxylic acids (Table 1). However, dissolution promotion is not tied strictly to the number of carboxyl moieties per molecule. For instance, 1,3,5-cyclohexanecarboxylic is only about half as efficient a dissolution promoter as cholic acid glutarate dimer despite the former having more carboxylic acid moieties per molecule. Moreover, looking at the monocarboxyl cholate derivatives, *f*(molar) tends to decrease giving increased dissolution promotion as the number of hydroxyl groups in the molecule increases. The greater effectiveness of cholic acid derivatives as dissolution promoters compared to other *tert*-butyl carboxylates without hydroxyls and the tendency for this effectiveness to increase with hydroxyl substitution may be tied to the ability of bile acids such as cholic acid to complex and disperse water-insoluble hydrophobic molecules.[18]

Lithographic contrast is one measure of the resolution power of a resist.[24] The contrast producing event in the P(NB/MA/AA)−*tert*-butyl carboxylate resists is a switch from an essentially hydrophobic state of the matrix to a hydrophilic one. This switch is achieved by transforming the *tert*-butyl carboxylic ester additives to the corresponding carboxylic acids through acidolytic deprotection by photogenerated acid. In the alkaline TMAH developer solution these new carboxylic acid groups produce ion sites along with the initially present polymer bound AA moieties, which both act as percolation sites. Consequently, the change in molar dissolution inhibition factor Δ*f*(molar) between a *tert*-butyl carboxylate and its corresponding free acid should be a measure of potential image contrast in solution containing the same mol % of different *tert*-butyl carboxylates. On this basis the most effective material is cholic acid glutarate dimer (Δ*f*(molar) = 6.05), which is 1.7−2.8 times more effective than monomeric cholates and 2−4 times more effective than cyclohexanecarboxylates (Table 1).

Similarly, the weight-based Δ*f* can predict the behavior of solutions containing the same wt % of different *tert*-butyl carboxylate. Table 1 lists the contrasts of films of P(NB/MA/TBA/AA) containing 25 wt % of select *tert*-butyl carboxylates. These data shows that there is a only a fair correlation between the observed contrasts and the Δ*f* values ($R^2 = 0.79$). The correlation between *f* values of the carboxylic acids and the maximum rate of dissolution of each film (R_{max}) is better ($R^2 = 0.89$). Partial deprotection of *tert*-butyl carboxylate moieties to form carboxylic acids could be one source of deviation from ideal behavior. Indeed, by using FT-IR spectroscopic monitoring, it was found that tri-*tert*-butyl 1,3,5-cyclohexanetricarboxylate undergoes acidolysis in a more effective fashion than *tert*-butyl cholates such as bis(*tert*-butyl 3α-yl,7α,12α-5β-dihydroxycholan-24-oate) glutarate (*tert*-butyl cholate glutarate dimer) (Figure 6). This presumably occurs as a consequence of the closer proximity of carboxyl groups in the 1,3,5-cyclohexanetricarboxylate moiety, which lowers the acidolysis temperature through an electron-withdrawing inductive effect. This is confirmed by thermogravimetric analysis (TGA) where the onset for thermolytic removal of isobutene for tri-*tert*-butyl 1,3,5-cyclohexanetricarboxylate (207 °C) was much lower than that of *tert*-butyl cholate (280 °C).

(21) Peterson, B. R.; Wallimann, P.; Carcanague, D. R.; Diederich, F. *Tetrahedron* **1995**, *51*, 401−421.

(22) Wang, Y.; Ikeda, T.; Ikeda, H.; Ueno, A.; Toda, F. *Bull. Chem. Soc. Jpn.* **1994**, *67*, 1598−1607

(23) The cloud point is a more complex value than log P_{oct} because it is governed by both the interactivity of the DI (i.e., solute−solute interactions) and its hydrophobicity (i.e., solute−water interactions). Because DI self-association probably parallels DI−matrix interactions, cloud point may be better suited as a predictive tool for dissolution inhibition.

(24) *Introduction to Microlithography, Theory, Materials and Processing*; Thompson, L. F., Willson, C. G., Bowden, M. J., Eds.; ACS Symposium Series 219; American Chemical Society: Washington, D.C., 1983, p 170.

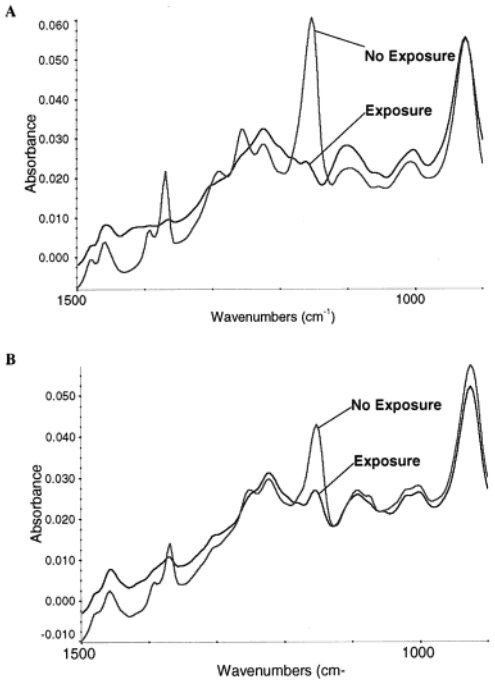

Figure 6. Infrared study of extent of resist deprotection for resist formulated with P(NB/MA/AA/TBA) exposure, 100 mJ/cm^2, 193 nm, and PEB of 150 °C, 90 s: (A) resist containing 25 wt % *tert*-butyl 1,3,5-cyclohexanetricarboxylate; (B) resist containing 25 wt % bis(*tert*-butyl 3α-yl,7α,12α-5*β*-dihydroxy-cholan-24-oate) glutarate.

Another important question in dissolution promotion is whether AA repeat units and acidolysis of *tert*-butyl ester additives are the only source of percolation sites for these resist systems. Indeed, films containing P(NB/MA) and 2 wt % of a PAG (bis-*tert*-butylphenyliodonium triflate) fail to dissolve after exposure. Films containing these components and 25 wt % *tert*-butyl cholate glutarate dimer undergo dissolution albeit at a rate approximately an order of magnitude slower and have a lower contrast (4.5) than those containing a P(NB/MA/AA) or P(NB/MA/TBA/AA) resin. This indicates that percolation through hydrolysis of the anhydride moiety is not as efficient as the percolation through nonhydrolytically formed polymer-bound carboxylic acid polymer.

The Effect of Resin Carboxylic Acid Content on Blending of Cholate with P(NB/MA/AA). A previous study[19] examining the level of interaction between $-CO_2H$ polymer-bound moieties and cholate DI's by $-OH$ FT-IR shifts in a matrix of P(NB/MA/AA) found that AA moieties tend to interact more strongly in the order *tert*-butyl deoxycholate > *tert*-butyl cholate > *tert*-butyl lithocholate> *tert*-butyl chenodeoxycholate = *tert*-butyl cholate glutarate dimer. Although the strength of these interactions does not correlate with dissolution inhibition, it does appear to play a role in the ability of a polymer matrix to accommodate large amounts of cholate DI's. Figure 7A,B shows that a larger proportion of acrylic acid repeat units in a resin leads to better blendability indicated by the greater linearity between log(*R*) and the DI loading. The superior ability of *tert*-butyl deoxycholate to be solubilized in a polymer matrix containing carboxylic acid moieties may explain the higher contrasts previously observed with such materials at high loadings.[11,12]

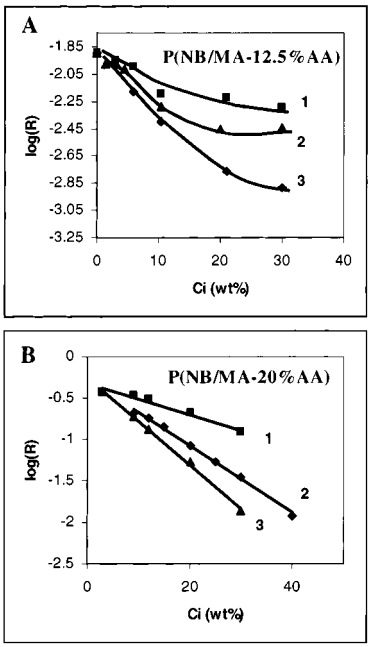

Figure 7. Comparison of loading capacity of different dissolution inhibitors in P(NB/MA/AA) resins with different loading capacities of carboxylic acid as measured from the plot of log(*R*) versus wt %.

Interaction of Photoacid Generators. *f* values were established for a variety of PAG's in P(NB/MA/AA) (12.5% AA), the same resin used to evaluate the *tert*-butyl carboxylates. Adjusting for molarity by using *f*(molar), it can be seen that these PAG's can impart a wide variance in dissolution inhibition (Table 2) [e.g., bis(*tert*-butylphenyl)iodonium tresylate (*f*(molar) = 7.6); tris(*tert*-butylphenyl)sulfonium perfluorooctanesulfonate (*f*(molar) = 1.9)].

As before, spectroscopic tools were used to investigate possible interactions of the additives with the matrix to see if these could contribute to the dissolution inhibition mechanism. FT-IR spectroscopy of films containing different PAG's in either a P(NB/MA), P(NB/MA/TBA), P(NB/MA/AA), or P(NB/MA/TBA/AA) resin did not show any significant band shifts of anhydride or *tert*-butyl carboxylate moieties indicative of PAG interaction. Possible band shifts of carboxylic acid moieties due to PAG interactions could not be observed owing to overlaps with the anhydride band. Consequently, a ^{13}C NMR spectroscopic experiment was done in which equimolar quantities of different PAG's were mixed with half the molar amount of either acetic acid or dimethyl succinic anhydride (Table 2). Confirming the FT-IR results, the carbonyls of dimethyl succinic anhydride did not show any peak shifts indicative of association (Table 2). However, all onium salt PAG's induced large upfield shifts (1.4−3.1 ppm) in the peak position for the carbonyl of acetic acid (177.3 ppm). By plotting the shifted peak positions (Table 2) versus the *f*(molar) for the series of homologous perfluoroalkylsulfonate anions[25] (i.e., triflate, nonaflate, and perfluorooc-

(25) The plot was done over a homologous series to avoid chemical shift changes induced by diamagnetic anisotropy effect, which might occur when using anions having greatly different structures (i.e., nonaflate vs perfluorobenzenesulfonate) or chromophores having different structures (i.e., tris(*tert*-butylphenyl)sulfonium vs bis(*tert*-butylphenyl)iodonium)

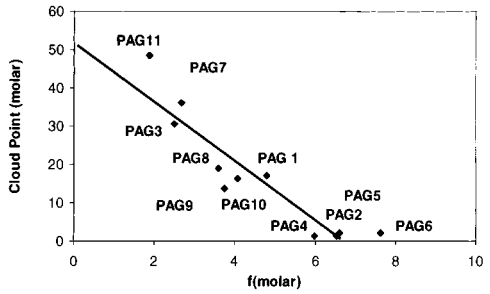

Figure 8. Plot of cloud point(molar) for PAG's versus *f*(molar) values in a P(NB/MA/AA) (12.5%) resin developed with 0.26 N TMAH

tanesulfonate), it is seen that both the bis(*tert*-butylphenyl)iodonium (R^2 = 0.95) and tris(*tert*-butylphenyl)-sulfonium (R^2 =: 0.92) show a good correlation of decreasing chemical shift with increasing *f*(molar). The upfield shift observed in these experiments would be consistent with breaking apart of the acidic acid dimer by complex formation with another molecule.[26] In the polymer matrix this would mean that onium salts having smaller anions associate more strongly with carboxylic acid moieties.

Cloud Point Measurements Done on PAG's. Cloud points for the different PAG's were measured in the same manner as for the *tert*-butyl carboxylates (vide infra) (Table 2). Figure 8 shows a plot of cloud point-(molar) versus *f*(molar) for perfluorinated onium salts indicating a good correlation (R^2 = 0.84) between increasing cloud point(molar) and decreasing *f*(molar). Interestingly, this means that perfluorinated PAG materials with large hydrophobic anions give far less dissolution inhibition than PAG's with small perfluorinated anions. This is in contrast to the *tert*-butyl carboxylates in which large hydrophobicity gave good dissolution inhibition. Additionally, it appears that the interaction of PAG's with the matrix leading to high dissolution inhibition factors is very susceptible to steric constraints as seen in Figure 9, which shows a plot of sulfonate molar volume versus *f*(molar). Since in the NMR experiments it was observed that onium salts with smaller anions tend to interact more strongly with carboxylic acid moieties, this is a good indication that PAG carboxylic acid interactions are primarily responsible for dissolution inhibition for these materials.

The good correlation between cloud point(molar) and *f*(molar) also indicates that in this instance the effect of perfluorinated anions predominates over differences caused by cation present in the PAG (i.e., tris(*tert*-butylphenyl)sulfonium vs tris(*tert*-butylphenyl)iodonium).[27]

This mechanism of interaction with carboxylic acid matrices appears to only hold for onium salt acid generators that have anions that are poor electron donors (e.g., BF_{4-}, $C_nF_{2n}SO_{3-}$, $C_6F_6SO_{3-}$, SbF_{6-}, etc). For the analogues containing more electron-rich sulfonate anions (e.g., camphorsulfonate) or covalent PAG's containing relatively electron-rich sulfonate moieties (e.g., bis(2,6-dinitro-α-ethyloxycarbonylbenzyl) 1,3-benzenesulfonate), high dissolution inhibition corresponds to high hydrophobicity (Table 2). These more electron-rich sulfonates may interact with the polymer resin by oxygen lone pair interactions in a manner analogous to diazonaphthoquinone novolak dissolution inhibition systems.[17b]

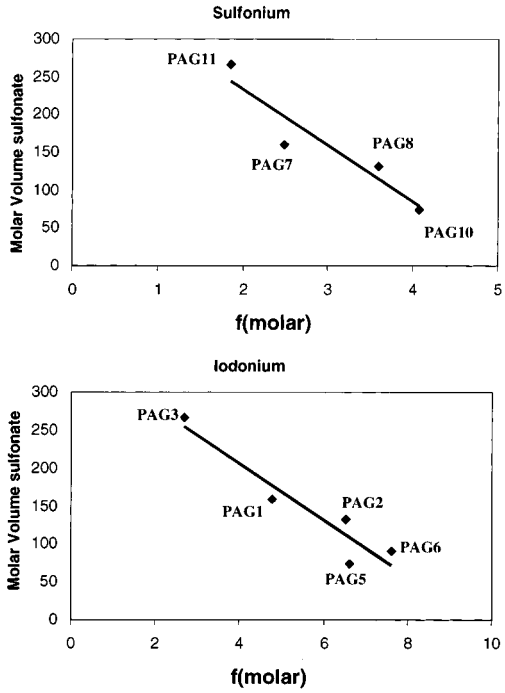

Figure 9. Plot of *f*(molar) vs the calculated molar volume of the sulfonate anion. Sufonium = tris(*tert*-butylphenyl)sulfonium salts; iodonium = bis(*tert*-butylphenyl)iodonium salts. Molar volumes were calculated using the program cited in ref 20.

Conclusions

The dissolution inhibition mechanism of *tert*-butyl carboxylates in various poly(norbornene−maleic anhydride−acrylate) resins appears to be mainly governed by hydrophobicity with only a small possible influence of hydroxyl anhydride interaction. This would be consistent with the behavior of certain steroidal molecules where van der Waals interactions determine the strength of complex formation. Although not directly implicated in dissolution inhibition, the interaction of resin-bound carboxylic acid moieties with hydroxyls of *tert*-butyl cholates is implicated in achieving good blendability of the DI with the resin. For PAG's based upon onium salts of perfluorinated anions, an interaction of carboxylic acid with PAG appears to be primarily responsible for dissolution inhibition. In this instance, PAG's with a large hydrophobic perfluorinated anion showing poor interaction with carboxylic acids give poor dissolution inhibition. The disruption of the interaction may be steric in nature, or alternatively may be caused by sequestration in the resin of PAG's with large surfactant-like perfluorinated anions. The PAG's with large hydrophobic perfluorinated anions also have little capacity to interact with the resin though van der Waals interactions owing to the low polarizability of perflu-

(26) Strothers, J. B. *Carbon-13 NMR Spectroscopy, Organic Chemistry, A Series of Monographs;* Academic Press: New York, 1972; p 297

(27) This said, there is a better somewhat better correlation of cloud point(molar) with *f*(molar) if one separates the onium salts according to cation type (i.e., tris(*tert*-butylphenyl)sulfonium, R^2 = 0.92; bis(*tert*-butylphenyl)iodonium, R^2 = 0.90). This is probably because of expected differences in steric size and hydrophobicity between the two cations.

orinated moieties. This is contrast to the large hydrophobic cholate dissolution inhibitors that do have a large capacity to interact by van der Waals interactions and indeed do show high dissolution inhibition. For other PAG's having more electron-rich sulfonate moieties, high dissolution inhibition appears to be better correlated with large hydrophobicity. In these PAG's the main interaction responsible for dissolution inhibition may be sulfonate lone pair interactions with the matrix.

Experimental Section

Synthesis. The syntheses of P(NB/MA/TBA/AA), P(NB/MA/TBA), P(NB/MA/AA), and P(NB/MA)[3,4] monomeric cholate dissolution inhibitors have been previously described.[11,12,19,28] The syntheses of *tert*-butyl cyclohexanecarboxylates, adamantanecarboxylate, and *n*-butyl malonate were done by a variation of the procedure already described for the cholate dissolution inhibitors starting from commercially available carboxylic acids. Starting materials, dry solvents, di-*tert*-butyl oxalate, di-*tert*-butyl malonate, and di-*tert*-butyl acetonedicarboxylate were obtained from the Aldrich Chemical Co.

Acid salts were either commercially available (triflate, nonaflate, perfluorooctanesulfonate) from Aldrich or Fluka or made by hydrolysis of the corresponding acid chloride removal of HCl and reaction of the crude acid with silver carbonate available from Aldrich in a manner similar to what has been previously described.[29] The synthesis of (2,6-dinitrobenzylethoxycarbonyl)benzyl 1,3-benzenesulfonate (**PAG12**) was done as previously described.[30]

Here follows two typical examples for the synthesis of *tert*-butyl carboxylates and a PAG:

Synthesis of Di-tert-butyl 1,4-Cyclohexanedicarboxylate (7). Ten grams of dry (dried under vacuum 50 °C overnight) 1,4-cyclohexanedicarboxylic acid (50/50 mixture of isomers) was dissolved in 150 mL of dry THF under argon and cooled to 0 °C. To the cooled solution was added dropwise 42.5 mL of trifluoroacetic anhydride while maintaining the addition rate such that the temperature did not rise above 10 °C. The mixture was allowed to warm to room temperature and stirred for 90 min. Then, the solution was cooled to 0 °C, and 45 mL of dry *tert*-butyl alcohol was added dropwise at a rate such that the temperature did not exceed 10 °C. The reaction mixture was stirred at 0 °C for 10 h. Fifty milliliters of concentrated aqueous NH_4OH was then added to the mixture at 0 °C, adjusting the addition rate such that the temperature did not exceed 10 °C. The solution was stirred at 0 °C for 24 h, and then 250 mL of ether and 250 mL of water were added giving a two-phase system. The ether phase was separated, washed three times with 50 mL of water, concentrated, and dried. Recrystallization was done by dissolving in a minimum of hot methanol (∼60 mL), adding water until cloudy, reheating until clear, and cooling to initiate final crystallization. The white crystals were collected and dried under vacuum (95% yield).

Synthesis of Tri-tert-butyl 1,3,5-Cyclohexanetricarboxylate (9). Ten grams of dry (dried under vacuum 50 °C overnight) 1,3,5-cyclohexanetricarboxylic acid was dissolved in 150 mL of dry THF under argon and cooled to 0 °C. To this was added dropwise 73.9 mL of trifluoroacetic anhydride while maintaining the addition rate such that the temperature did not rise above 10 °C. The mixture was then allowed to warm to room temperature and stirred for 90 min. The solution was then cooled to 0 °C, and 199 mL of dry *tert*-butyl alcohol was added dropwise at a rate such that the temperature did not exceed 10 °C. The reaction mixture was stirred at 0 °C for 10 h. One hundred-seventy milliliters of concentrated aqueous NH_4OH was then added to the mixture at 0 °C adjusting the addition rate such that the temperature did not exceed 10 °C. The solution was stirred at 0 °C for 24 h, and then 650 mL of both ether and water were added producing a two- phase system. The ether phase was separated out and washed three times with 50 mL of water and then concentrated and dried. The residue was recrytallized three times by dissolving into 50 mL of acetone and adding 20 mL of water. The final product was dried under vacuum overnight to give white crystals (27% yield).

Synthesis of Bis(tert-butyl 3α-yl,7α,12α-5β-dihydroxycholan-24-oate) Glutarate (6). A solution was prepared under argon consisting of *tert*-butyl cholate (5.00 g, 1.08 mmol) and *N*-methyl morpholine (1.83 g, 1.98 mL, 1.81 mmol) dissolved in 15 mL of dry tetrahydrofuran. To this solution at was added dropwise, over a period of 15 min, a solution consisting of glutaryl dichloride (0.91 g, 0.69 mL) dissolved in 15 mL of dry THF, making sure that the temperature did not exceed 40 °C. The reaction mixture was then heated to 60 °C and kept at this temperature overnight (∼13 h). The reaction mixture was then cooled to room temperature, and 30 mL of both methylene and water were added. After this two-phase system was shaken, the water layer was removed and the organic layer was extracted with two 50 mL aliquots of 4% acetic acid. The organic layer was then washed with five 10 mL aliquots of water and dried over anhydrous magnesium sulfate, and after filtration the solvents were removed under vacuum. The residual foam was recrystallized by dissolving in 20 mL of hot acetonitrile and allowed to cool to 5 °C. A second recrytallization was done with 10 mL of solvent, giving white crystals (48% yield).

Synthesis of Tris(tert-butylphenyl)sulfonium Perfluorobenzenesulfonate (PAG8). A suspension consisting of 1 g (2.14 mmol) of tris(*tert*-butylphenyl)sulfonium tetrafluoroborate in 20 mL of ethyl acetate was made. This suspension was added with stirring to a solution consisting of 1.42 g (4.28 mmol) silver perfluorobenzenesulfonate dissolved in 20 mL of water. After 2 h of stirring the suspended tris(*tert*-butylphenyl)-sulfonium tetrafluoroborate salt dissolved. The organic layer was separated from the aqueous layer, diluted into 20 mL of additional ethyl acetate, and shaken with two 20 mL aliquots of fresh aqueous silver perfluorobenzenesulfonate. The organic layer was then shaken with six 20 mL aliquots of water. The organic solvent and residual water were removed under vacuum giving 1.51 g of crude product. This crude product was recrystallized three times from a mixture of methylene chloride and ethyl acetate to give white crystals (74% yield).

Dissolution Rate Monitoring Studies. Formulation of resists based on P(NB/MA/AA) (12.5 or 20 wt %) was done by blending with varying amounts of additive (*tert*-butyl carboxylate, carboxylic acid, or PAG) (0−30 wt %) as a 13 wt % solution in propyleneglycol methyl ether acetate.

Processing of 193 nm Test Resists Formulated with Either P(NB/MA/TBA/AA). Silicon wafers were spin-coated with resist and baked at 150 °C for 90 s. The spin speed was 2000−3000 rpm to get a nominal resist thicknesses of 0.40−0.36 μm. The resist thickness was measured by a Nanospec AFT thickness gauge using a refractive index of 1.51. The dissolution rate experiments were done with a Perkin-Elmer 5900 Development rate monitor interfaced with a DREAMS application version 3.00D DRM software package. Development was done at 25 °C with OPD262 developer from Arch Chemicals. The R_{max} experiments were done similarly by using a resist formulated with P(NB/MA/TBA/AA) (30% TBA and 2% AA) and containing 25 wt % of one of the DI's indicated in Table 1 and 2 wt % of tris(*tert*-butylphenyl)sulfonium nonaflate. A flood exposure of 100 mJ/cm^2 at 193 nm was employed using a LPX 100 Lambda Physik excimer laser interfaced with a Karl Suss Contact printer.

Cloud Point Determinations. Cloud point measurements were done by slowly adding distilled water into a solution consisting of 0.01 g of a DI in 1 mL of acetone until a persistent

(28) Bonar-Law, R. P.; Davis, A. P.; Scanners, J. K. M. *J. Chem. Soc., Perkin Trans. 1* **1990**, 2245.

(29) Taylor, G.; Stillwagon, L. E.; Houlihan, F. M.; Sogah, D. Y.; Hertler, W. R. *Chem. Mater.* **1991**, *3*, 1021

(30) (a) Houlihan, F. M.; Chin, E.; Nalamasu, O.; Kometani, J. M.; Neenan, T. X.; Pangborn, A. *Proceedings of the International Society for Optical Engineering; Advances in Resist Technology and Processing XIII* **1994**, *2195*, 137. (b) Houlihan, F. M.; Chin, E.; Nalamasu, O. U.S. Patent 5, 830, 619, Nov 3, 1998.

cloudiness (solid formation) was observed; it is expressed in vol % of acetone.

General Spectroscopic Procedures. Films of polymers, dissolution inhibitors, and blends were cast onto 2 mm thick NaCl disks from solutions (approximately 15 wt %) prepared in acetone or in propylene glycol methyl ether acetate (PGMEA). Films were dried in a 100 °C oven for 10 min prior to the acquisition of Fourier transform-infrared (FT-IR) spectra. Films cast from PGMEA were subsequently dried in vacuo at 60 °C for 15 min. FT-IR spectra were obtained using a Nicolet Magna System 560. Generally, FT-IR spectra were obtained over 80 s with a total of 64 acquisition scans using 8 kilobytes of data and zero filling to 16 kilobytes prior to Fourier transforming the data. The spectra were all baseline corrected manually using a linear correction with zero points chosen to be at the extremes of the spectrum (4000 and 650 cm^{-1}) and at the boundaries of the three regions of interest, OH stretch (3700−3060 cm^{-1}), CH stretch (3060−1920 cm^{-1}), and the C═O stretch (1920−1530 cm^{-1}). The FT-IR spectral data in the region from 3060 to 2430 cm^{-1} (CH stretch) obtained from a blend of DI and polymer was fit to a linear combination of the spectral region obtained from the pure DI and the pure polymer. The coefficients obtained from the fit were used to scale the entire spectrum of the pure components. Addition of these two scaled spectra gave rise to a spectrum that was used as the reference to which the blend spectrum was compared. Peak positions were determined after smoothing the data to reduce artifacts due to noise.

^{13}C NMR spectra were obtained using a Bruker AM360 NMR spectrometer operating at 90.56 MHz. Pulse widths of 3 ms (corresponding to a 20° flip angle) were used at a 4 s repetition rate. Typically 1000 transients were collected using 32 kilobytes of data points and were transformed using exponential line broadening of 1 Hz. The digital resolution was 1.4 Hz/point. Chemical shifts were referenced to either tetramethylsilane at 0.00 ppm or to the $CDCl_3$ triplet centered at 77.0 ppm.

NMR samples for interaction studies with PAG's were prepared by dissolving 0.1 mmol of photoacid generator in 0.5 mL of a stock solution containing either 0.05 mmol acetic acid in $CDCl_3$or 0.05 mmol of 2,2-dimethylsuccinic anhydride in $CDCl_3$. Proton NMR spectra were acquired at 360.134 MHz. Integrated peak areas were used to determine relative concentration of PAG to the model compound being observed. Carbon NMR spectra were acquired at 90.56 MHz using a Bruker AM360 NMR Spectrometer. All shifts are reported relative totetramethylsilane with a digital resolution of 0.02 ppm/point

Thermolysis Studies. TGA analysis was done on ∼3 mg samples under nitrogen using a Perkin-Elmer 7 series thermal analysis system set at a heating rate of 10 °C per min.

CM000385K